structural interpretation is not possible, a change in structure will almost surely show up as a change in CD.

One other useful application of CD is in studying the binding of small molecules to proteins or nucleic acids. This works best with a small molecule that absorbs visible light. An optically active small molecule may show a change in CD upon binding to a macromolecule, either because of electronic interactions with its binding site or because it may undergo a conformational change when it binds. These changes can be detected easily because most common biopolymers have no CD for visible light.

It is especially convenient to study optically *inactive* small molecules. Here an induced CD will usually occur upon binding, for the same reasons just mentioned for optically active small molecules. However, CD measurements in the absorption band of the small molecule will reflect only properties of the bound material. This makes it easier to determine whether there is a class of essentially equivalent binding sites, and to study the number of bound ligands. If all sites are very similar, the induced CD of the small molecule will be given by $\theta = C_b[\theta_b]l \cdot 100$, where C_b is the concentration of bound small molecules, $[\theta_b]$ is the CD of bound species (determined by saturation of a sample of small molecules with excess polymer), and l is the path-length. Once $[\theta_b]$ is known, C_b can be calculated from the measured θ. From this, binding constants and (ultimately) apparent thermodynamic data on the binding equilibrium are obtained.

Several factors contribute to the induced CD of a small molecule when it is bound to an asymmetric site on a polymer. The effect of the environment will show up as one-electron-type contributions. In addition, coupled oscillator terms can yield strong induced CD if the energy levels of protein or nucleic acid chromophores are similar to the energy levels of the small molecule. For example, much of the optical activity of bound heme groups in hemoglobins can be accounted for by interaction with nearby tyrosine residues of the protein.

Variations of optical activity measurements

In a magnetic field, optical activity becomes an even more complex phenomenon. Even many optically inactive molecules can show CD and ORD if a magnetic field is present. Optically active molecules show normal CD bands but, in addition, other magnetically induced bands appear. Work in the areas of magnetic ORD and magnetic CD spectroscopy is still in earlier stages of development than that in normal CD. In the future, many useful applications of magnetic CD and ORD are likely to appear.

The operators that lead to normal optical activity are actually tensors, rather than scalars. In normal isotropic solution, the random orientations of molecules average over the tensor properties, and the resulting measured quantity is the trace (sum of diagonal elements) of the optical activity tensor. More information is potentially available about the system if individual elements of the tensor are measured. This can be done by orienting the system. Such experiments are technically very

Sct 2-9

challenging because the oriented system now demonstrates linear dichroism as well as circular dichroism, and the two effects must be sorted out. When all of this is done, a more complete picture of the nature of polymer electronic states is revealed.

If an optically active system is fluorescent (see the next section), two additional aspects of optical activity can be measured. Suppose that circularly polarized exciting light is used, but all emitted light is detected. The intensity of emitted light is proportional to the amount of light absorbed. Thus the difference in emitted intensities when right-hand and left-hand circularly polarized light is used will yield the differential absorbance (that is, the CD) of only the fluorescent chromophores. Thus, for example, if a protein contained two tryptophans, only one of which was fluorescent, normal CD would give the sum of their optical properties. Fluorescence-detected CD would provide the CD of one individual tryptophan; then the CD of the other tryptophan could be obtained by difference. Alternatively, one can use unpolarized exciting light, but measure the difference in the extent to which left-hand and right-hand circularly polarized light is emitted. This approach yields the CD of a chromophore in its excited-state configuration, in distinction to all other CD measurements, which essentially monitor ground-state configurations (see Steinberg, 1978).

One final variation on optical activity is CD in the infrared region of the spectrum. This technique is still in its infancy, but it shows promise as a new structural tool for small and large molecules.

8-2 FLUORESCENCE SPECTROSCOPY

Light emission can reveal properties of biological molecules quite different from the properties revealed by light absorption. The process takes place on a much slower time scale, allowing a much wider range of interactions and perturbations to influence the spectrum.

Basic principles of fluorescence

Consider a hypothetical molecule with two energy levels, S_b and S_a:

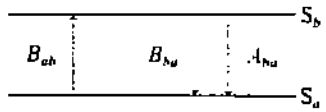

In Section 7-1, we showed that light of radiation density $I(\nu)$ induces the transition from S_a to S_b at a rate of B_{ab} per molecule. The radiation-induced process $S_b \rightarrow S_a$ occurs at exactly the same rate: thus $B_{ab} = B_{ba}$. If the system originally contains n_a molecules in state S_a and n_b in state S_b, then the net rates of conversion are $n_a B_{ab} I(\nu)$ and $n_b B_{ba} I(\nu)$, respectively. At equilibrium, these rates must be equal. Hence $n_a B_{ab} I(\nu) =$

$n_b B_{ba} I(\nu)$, or $n_a = n_b$, independent of radiation density. Unfortunately, this is an absurd result. Without light, virtually all molecules should be in the ground state, S_a. At low light intensities, one hardly expects a major perturbation of the equilibrium values of n_a and n_b. These values are derivable from statistical mechanics. Ignoring degeneracy, a simple Boltzmann factor applies:

$$n_a/n_b = e^{-(E_a - E_b)/kT} = e^{+h\nu/kT} \tag{8-27}$$

where h is Planck's constant.

It was Albert Einstein who first noted that, to resolve this discrepancy, one could postulate a rate of spontaneous emission of a photon from state S_b. The rate of this process (A_{ba}) should be independent of $I(\nu)$. When spontaneous emission is included and the rates of interconversion of S_a and S_b are set equal at equilibrium, the result is

$$n_a/n_b = [B_{ba} I(\nu) + A_{ba}]/B_{ab} I(\nu) = 1 + A_{ba}/B_{ab} I(\nu) \tag{8-28}$$

By setting Equations 8-27 and 8-28 equal, we can evaluate A_{ba}. To do this, we must first insert for $I(\nu)$ the radiation density expected for a black body[1] at temperature T:

$$I(\nu) = 8\pi h\nu^3/c^3(e^{h\nu/kT} - 1) \tag{8-29}$$

With this substitution, Equation 8-28 becomes

$$n_a/n_b = 1 + A_{ba}/B_{ab} I(\nu) = 1 + A_{ba}(e^{h\nu/kT} - 1)/8\pi h\nu^3 c^{-3} B_{ab} \tag{8-30}$$

When this value is set equal to $e^{h\nu/kT}$ (from Eqn. 8-27), the result for A_{ba} is

$$A_{ba} = 8\pi h\nu^3 c^{-3} B_{ab} \tag{8-31}$$

Note that this expression depends on the cube of the frequency. This means that, at short wavelengths, A_{ba} is much larger than B_{ab}. Essentially all emission is spontaneous. Earlier (Eqn. 7-29) we showed that $B_{ab} = (2\pi \cdot 3h^2)D_{ab}$. Thus we can obtain

$$A_{ba} = (32\pi^3\nu^3\ 3c^3h)D_{ab} \tag{8-32}$$

Because the dipole strength (D_{ab}) and the frequency (ν) usually can be measured from the absorption spectrum, the rate of spontaneous emission can be determined without performing an emission measurement at all. In the absence of radiation or any other perturbations or interactions, the rate of deexcitation of molecules initially in state S_b will be

$$dn_b/dt = -A_{ba} n_b \tag{8-33}$$

The solution of this differential equation is $n_b(t) = n_b(0)e^{-A_{ba}t}$, where $n_b(0)$ is the concentration of excited states at zero time. Hence we can define the radiative lifetime of state S_b as

$$\tau_R = 1/A_{ba} \tag{8-34}$$

The dipole strength D_{ab} is a direct measure of the intensity of a spectral absorption. From Equation 8-32, it is clear that D_{ab} and A_{ba} are proportional. Thus Equation 8-34 indicates that the stronger the absorption of a given isolated molecule, the more rapid the emission of fluorescent radiation. Note carefully that Equation 8-34 is valid only so long as the same electronic state that absorbed the radiation is subsequently emitting it. This is not always the case. More elaborate versions of Equation 8-34 exist to handle such complexities as vibronic bands within electronic transitions.

In reality, the actual observed lifetime of an excited singlet state is rarely as long as the radiative lifetime computed by Equation 8-34. This is because the excited state can lose its energy through many other processes besides direct emission of light (Fig. 8-11). We shall discuss each process in some detail because each potentially can yield useful information on biological structures.

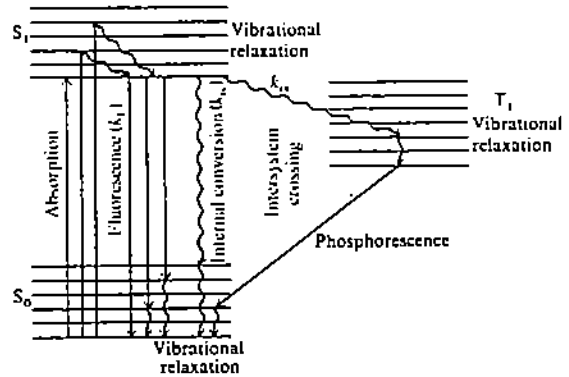

Figure 8-11

Pathways for production and deexcitation of an excited state. [After C. R. Cantor and T. Tao, in *Procedures in Nucleic Acid Research*, vol. 2 (New York: Harper & Row, 1971), p. 31.]

[1] At equilibrium, the emission and absorption of radiation density must be equal. For an object at temperature T, the radiation density required for equilibrium is given by Equation 8-29. [See R. P. Feynman, R. B. Leighton, and M. Sands, *The Feynman Lectures on Physics*, vol. 1 (Reading, Mass.: Addison-Wesley, 1963), chaps. 41–42.]

The intrinsic fluorescence rate constant (k_F) can be evaluated from the preceding discussion as

$$k_F = A_{ba} = 1/\tau_R \tag{8-35}$$

as long as stimulated emission is negligible. The nonradiative processes that compete with fluorescence (and the rate constants that characterize them) include internal conversion (k_{ic}), intersystem crossing (k_{is}), and quenching of various types [k_q(Q)]. All of these processes compete directly to depopulate the excited singlet state. Therefore, the fraction of excited singlets that become deexcited through fluorescence (called the fluorescence quantum yield, ϕ_F) is simply

$$\phi_F = k_F/[k_F + k_{ic} + k_{is} + k_q(Q)] \tag{8-36}$$

The fluorescence quantum yield (ϕ_F) is equal to the ratio of photons emitted to photons absorbed by the system.

Factors governing fluorescence intensity

We now examine in more detail the factors that affect the intensity of fluorescence.

1. Internal conversion, occurring at a rate k_{ic}. In this process, excitation energy in S_b is lost by collision with solvent or by dissipation through internal vibrational modes. In general, k_{ic} will increase as the temperature is raised. Therefore, the observed fluorescence will decrease with increasing temperature. This intrinsic temperature dependence is not found in the other spectroscopic phenomena we have discussed. It can seriously complicate attempts to use fluorescence to monitor thermally induced macromolecular conformation changes.

2. Deexcitation resulting from collisions or complexes with solute molecules (Q) capable of quenching the excited state, occurring at a rate k_q(Q). Unlike all the other processes, quenching can (in principle) be a bimolecular step if collisions are involved.

$$S_b + Q \xrightarrow{k_q} S_a + Q \tag{8-37}$$

Because Q usually is in vast molar excess over S_b, the actual observed rate is pseudo first order. The value of k_q can be measured by varying the concentration of quencher, (Q), and then observing the effect on ϕ_F. Aromatic chromophores usually have radiative lifetimes in the range of 1×10^{-9} to 100×10^{-9} sec. Therefore, quenching processes must be quite effective to compete. Common quenchers, such as O_2 and I^- ion, deexcite essentially every time they collide with an excited singlet. Their rates are limited only by diffusion. At millimolar concentrations of quencher, collisions can approach rates of 10^8 sec^{-1}. Therefore, appreciable quenching is observed.

3. Intersystem crossing, occurring at a rate of k_{is}. In this process, the nominally forbidden spin exchange converts an excited singlet into an excited triplet state. That state can, in turn, convert to the ground singlet state (S_a), either by phosphorescence (emission of a photon) or by internal conversion. The triplet state generally is lower in energy than the excited singlet. Hence, phosphorescence occurs at longer wavelengths and can easily be resolved from fluoresence.

   The intensity for direct singlet–triplet absorption is extremely small. Therefore, triplet states usually can be seen easily only by emission spectroscopy. Another consequence of the low absorption intensity is that (as described by Eqn. 8-34) it will lead to an extremely long radiative lifetime for the triplet state. The lifetime is often in seconds or longer, rather than in the nanoseconds found for singlets. This means that collisions with quenchers or internal conversion can compete all too effectively with phosphorescence. Thus, in solution, phosphorescence rarely is observed. One usually must use rigid glasses at low temperature and must exclude oxygen fairly rigorously in order to see useful phosphorescence intensities. Because these conditions are rather far removed from the biological state, we shall concentrate on fluorescence methods rather than phosphorescence.

Because of all the nonradioactive processes just described, an excited singlet will decay faster than indicated by its radiative lifetime. The kinetic equation describing the decay of the concentration of excited singlets, ($S_b(t)$), is constructed by adding all parallel deexcitation pathways:

$$-d(S_b)/dt = [k_F + k_{ic} + k_{is} + k_q(Q)](S_b) \tag{8-38}$$

This equation has the solution

$$(S_b(t)) = (S_b(0))e^{-t/\tau_F} \tag{8-39}$$

where ($S_b(0)$) is the concentration at time zero, and τ_F is the observed fluorescence decay time:

$$\tau_F = [k_F + k_{ic} + k_{is} + k_q(Q)]^{-1} \tag{8-40}$$

Combining the definitions of τ_F, τ_R, and ϕ_F, we obtain

$$\phi_F = \tau_F/\tau_R \tag{8-41}$$

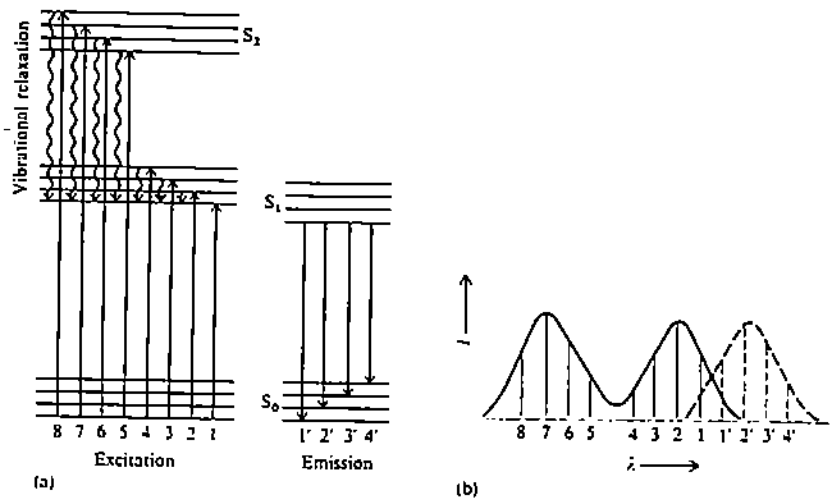

Figure 8-12

Excitation and emission of fluorescence. (a) Energy levels. (b) Spectra. Note that nonradiative transitions relax S_2 to S_1 much faster than any of the deexcitation processes can return S_1 to the ground state (S_0).

Because τ_R can, in principle, be calculated from the absorption spectrum, a measurement of the fluorescence decay rate (τ_F) is equivalent to a measurement of the quantum yield (ϕ_F).

Thus far we have considered only a single vibronic level of S_a and S_b. Figure 8-12 shows schematically the effect of other vibronic and electronic levels. Internal conversion between higher singlets, such as $S_c \rightarrow S_b$, is much faster than the rates we have considered up to now. Similarly, vibrational relaxation from excited vibrational levels of each electronic state to the ground vibrational level is much faster than photon emission. The result is that all observed fluorescence normally originates from the lowest vibrational level of the lowest excited singlet state. This observation has several important implications.

The spectrum of emitted light should be independent of the excitation wavelength.

Most or all of the fluorescence spectrum will be shifted to lower energies (longer wavelengths) than the longest-wavelength absorption band.

The shape of the emission band will be approximately a mirror image of the longest-wavelength absorption band (Fig. 8-12), providing that the vibronic structures of S_b and S_a are very similar.

The simple arguments shown in Figure 8-12 would predict that the zero–zero transitions in absorption [$S_a(v = 0) \rightarrow S_b(v = 0)$, line 1] and emission [$S_b(v = 0) \rightarrow S_a(v = 0)$, line 1'] should occur at the same wavelength. In solution, this usually is not the case. The absorption process occurs on such a short time scale that the environment can be considered fixed. Therefore, $S_a(v = 0) \rightarrow S_b(v = 0)$ corresponds to the energy difference with the solvent oriented in a favorable way about the ground-state configuration. If, after excitation, the solvent has time to reorient before emission, then $S_b(v = 0) \rightarrow S_a(v = 0)$ corresponds to the energy difference between the states while solvent is oriented favorably about the excited state. There is no reason why these energy differences must be the same and, in fact, either one could be larger. This effect leads to the shift in zero–zero frequencies called the Stokes shift.

Experimental measurements

Figure 8-13 shows a typical experimental arrangement for the measurement of fluorescence. This setup is used in two modes. With the excitation monochrometer M1 fixed, the emission monochrometer M2 can be scanned: this procedure yields an emission spectrum, the wavelength distribution of light emitted by the excited singlet. Alternatively, M2 can be fixed and M1 varied: this procedure produces an excitation spectrum. Because all states within or above S_b rapidly decay to the ground vibronic level of S_b before emission, the excitation spectrum of a pure compound should have exactly the same shape as the absorption spectrum.

With the simple apparatus shown in Figure 8-13, the single-beam arrangement leads to distortions in both excitation and emission spectra. The distortion in excitation spectra occurs because the lamp does not emit equal radiation intensities at all wavelengths. The distortion in emission spectra is mainly the result of frequency-dependent sensitivity of the detector. To correct for these phenomena, many spectrofluorimeters in current use are considerably more complex than that shown in Figure 8-13, but the basic principles remain the same.

One quantity frequently desired is the fluorescence quantum yield, ω_F—the fraction of excited singlets that decay by fluorescence. Absolute measurements of ϕ_F are quite difficult, as the following argument demonstrates. The number of excited molecules created by incident light of intensity I_0 is proportional to the number of excited photons. This quantity can be measured at wavelength λ_e by the decrease in light intensity as given by the Beer–Lambert law. Equation 7-33 can be written as

$$I = I_0 e^{-2.303\varepsilon(\lambda_e)Cl}$$

where $\varepsilon(\lambda_e)$ is the extinction coefficient at the exciting wavelength, C is the concentration of absorbing molecules, and l is the path length. For the low absorbances typically

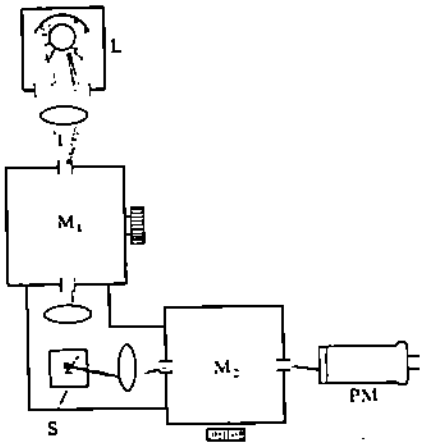

(a)

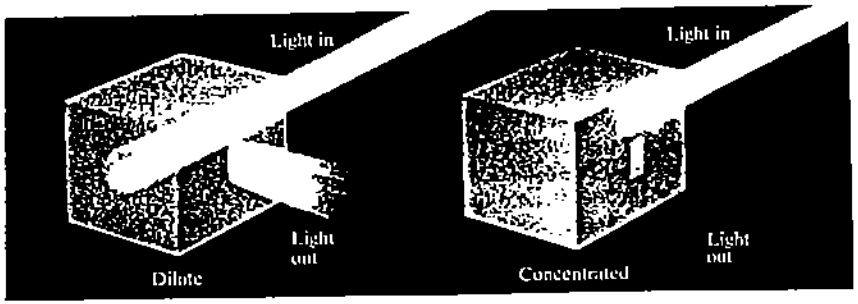

(b)

Figure 8-13

Steady-state fluorescence measurements. (a) Schematic diagram of a fluorescence spectrometer. M_1 is the excitation monochrometer. M_2 the emission monochrometer. L the light source, PM a photomultiplier detector, and S the sample. (b) An enlarged view of the sample chamber, showing the origins of the inner filter effect.

used in fluorescence, the exponential can be expanded to yield

$$I = I_0[1 - 2.303\varepsilon(\lambda_e)Cl]$$

The concentration of excited molecules will be proportional to the light intensity absorbed:

$$I_0 - I = 2.303\varepsilon(\lambda_e)ClI_0$$

The intensity of emission from one molecule at a particular wavelength λ is governed by the product of three factors: $\phi_F f(\lambda)d$, where ϕ_F is the probability of emitting at all; $f(\lambda)$ is the fraction of total emission that occurs at wavelength λ; and d is the fraction of radiation emitted at λ actually collected by the detector.

The actual observed emission intensity will be given by the product of absorption and emission probabilities:

$$F(\lambda) = 2.303\varepsilon(\lambda_e)ClI_0\phi_F f(\lambda)d = \varepsilon(\lambda_e)\phi_F f(\lambda)CI_0k \qquad (8\text{-}42)$$

where we have lumped together proportionality constants and the factors l and d that depend on experimental geometry into a single constant k. Integration of Equation 8-42 over λ results in a quantity proportional to the number of excited singlets. However, to determine the quantum yield ϕ_F, we must also know the absolute intensity of the exciting light, I_0, and the constant k.

In practice, rather than face all these complications, one measures relative quantum yields. A standard—such as quinine sulfate in 1 N H_2SO_4 ($\phi_F = 0.70$), or fluorescein in 0.1 N NaOH ($\phi_F = 0.93$)—is used to calibrate the instrument. The integrated fluorescence from Equation 8-42 is compared for the sample and for the standard after adjusting concentrations so that εC for both is the same.

An alternative to quantum yield measurements, suggested by Equation 8-41, is to measure decay rates. Conceptually, the simplest way to do this is to excite the sample with a short (~ 1 nsec) pulse of light and directly monitor the emission as a function of time. The intensity of light, $I(t)$, emitted at time t after the pulse will be proportional to the rate of decay of excited singlets and to the fraction of singlets that decay by fluorescence:

$$I(t) \propto \phi_F(S_b)/dt = (S_b(0))(\phi_F/\tau_F)e^{-t/\tau_R} = k_F(S_b(0))e^{-t/\tau_R} \qquad (8\text{-}43)$$

where we have inserted Equation 8-39 to compute $d(S_b)/dt$, and have used Equations 8-35 and 8-41 to remove ϕ_F and τ_R. Although it is possible to monitor kinetics directly, indirect methods usually are used to achieve the same effect. Figure 8-14 shows a typical result, obtained by the method of single-photon counting. The single exponential behavior predicted by Equation 8-43 is quite evident.

Suppose that a sample contains more than one fluorescent component. Now the emission spectrum will not be a constant. Rather, it will depend on the choice of

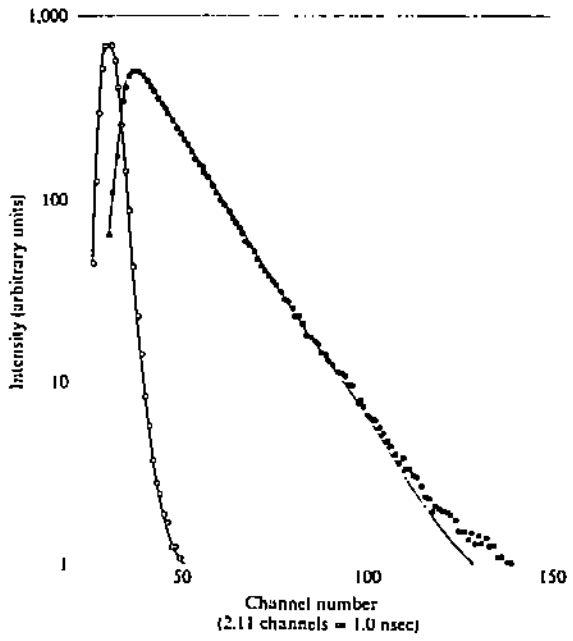

Figure 8-14

Fluorescence decay of the Y base in yeast $tRNA^{Phe}$. The black line shows the exciting pulse. The gray line through the fluorescence observations was generated from a knowledge of the shape of the exciting pulse and the assumption that the excited singlet state decays as a single exponential with $\tau_F = 6.2$ nsec. [After C. R. Cantor and T. Tao, in *Procedures in Nucleic Acid Research*, vol. 2 (New York: Harper & Row, 1971), p. 31.]

exciting wavelengths. For a mixture of two components (1 and 2), we have

$$F(\lambda) = [\varepsilon_1(\lambda_e)\phi_{1F}f_1(\lambda)C_1 + \varepsilon_2(\lambda_e)\phi_{2F}f_2(\lambda)C_2]I_0k \qquad (8\text{-}44)$$

where all quantitites are defined as in Equation 8-42. Similarly, the excitation spectrum will not be simply the sum of the two absorption spectra, because of weighting factors that depend on the quantum yield and wavelength dependence, $f_1(\lambda)$ and $f_2(\lambda)$, of fluorescence of each component. If the emission spectra of the two components overlap, the fluorescence decay will no longer be a single exponential. A sum of

exponentials will be observed:

$$I(t) = A_1e^{-t/\tau_{1F}} + A_2e^{-t/\tau_{2F}} \qquad (8\text{-}45)$$

The individual amplitudes (A_1 and A_2) will be weighted by the concentrations of the components.

One critical difference between steady-state and kinetic measurements of fluorescence cannot be ignored. The value of τ_F determined from Equation 8-43 will not be a function of concentration if the sample is a single pure species. In contrast, *Equation 8-42 holds only for optically thin samples* (absorbance at λ_e less than 0.03). In practice, if fluorescence is measured as a function of concentration, the observed intensity in an apparatus such as that shown in Figure 8-13 is linear with C when C is small, then saturates as C increases; and finally (at large enough C), $F(\lambda)$ actually decreases with increasing concentration. The origin of this inner filter effect is shown in Figure 8-13b. All the light is absorbed near the front surface of the cell, and most of the light emitted from this region is not collected by the exit slit.

Properties of typical fluorescent groups

Table 8-2 shows fluorescence characteristics of the chromophores found in proteins and nucleic acids. By and large, quantum yields are low and lifetimes are short. The experimental sensitivity, which will be governed by the product of ϕ_F and ε_{max} (Eqn. 8-42), is low. These are not ideal samples for experimental measurements. Figure 8-15 compares the fluorescence of a typical protein with that expected from

Table 8-2
Fluorescence characteristics of protein and nucleic acid constituents and coenzymes

		Absorption		Fluorescence[a]			Sensitivity
Substance	Conditions	λ_{max} (nm)	$\varepsilon_{max} \times 10^{-3}$	λ_{max} (nm)	ϕ_F	τ_F (nsec)	$\varepsilon_{max}\phi_F \times 10^{-3}$
Tryptophan	H_2O, pH 7	280	5.6	348	0.20	2.6	11.
Tyrosine	H_2O, pH 7	274	1.4	303	0.14	3.6	2.0
Phenylalanine	H_2O, pH 7	257	0.2	282	0.04	6.4	0.08
Y base	Yeast $tRNA^{Phe}$	320	1.3	460	0.07	6.3	0.91
Adenine	H_2O, pH 7	260	13.4	321	2.6×10^{-4}	<0.02	0.032
Guanine	H_2O, pH 7	275	8.1	329	3.0×10^{-4}	<0.02	0.024
Cytosine	H_2O, pH 7	267	6.1	313	0.8×10^{-4}	<0.02	0.005
Uracil	H_2O, pH 7	260	9.5	308	0.4×10^{-4}	<0.02	0.004
NADH	H_2O, pH 7	340	6.2	470	0.019	0.40	1.2

[a] Values shown for ϕ_F are the largest usually observed. In a given case actual values can be considerably lower.

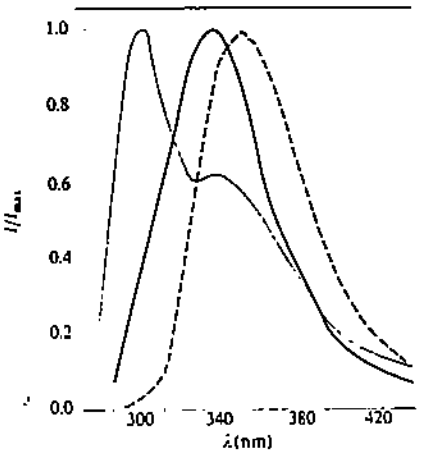

Figure 8-15

Normalized fluorescence emission spectra, produced by excitation at 240–250 nm of human serum albumin (*solid line*), tryptophan alone (*dashed line*), and an 18:1 molar ratio of tyrosine to tryptophan (*colored line*). The latter sample approximates the relative occurrence of these amino acids in the protein. Note that, except for a spectral shift, the spectrum of the protein closely resembles that of pure tryptophan. [After J. W. Longworth, in *Excited States of Proteins and Nucleic Acids*, ed. R. F. Steiner and I. Weinryb (New York: Plenum Press, 1971).]

individual amino acids. In most proteins, the fluorescence is dominated by tryptophan. Although tyrosine is a weaker emitter, one might expect it to contribute significantly because it usually is present in larger numbers. However, tyrosine usually is quenched by any nearby tryptophans because of energy-transfer effects to be discussed later.

The common nucleic acid bases have almost undetectably weak fluorescence—although a few unusual ones, such as the Y base, are intense enough to permit convenient study. This weak intrinsic fluorescence seems discouraging, but it is a blessing in disguise for many studies. The approach is to add a fluorescent probe to the system. This can be done by finding an intense fluorescent chromophore that binds at some specific site, or by covalently attaching such a chromophore. If the probe is properly placed, a variety of types of structural information can be obtained. Usually the probe is chosen so that it can be excited by light that only the probe (not the macromolecule) can absorb. In this case, the macromolecule is invisible, and all information relates to the probe molecule. Table 8-3 summarizes the properties of a few common probes (Fig. 8-16). Notice that the relative experimental sensitivity ($\epsilon_{max}\phi_F$) shown in the table is much higher than that of most intrinsic protein or nucleic acid constituents.

Sensitivity of fluorescence to the environment

Fluorescence generally is much more sensitive to the environment of the chromophore than is light absorption. Therefore, fluorescence is a most effective technique for following the binding of ligands or conformational changes. The sensitivity of fluorescence is a consequence of the relatively long time a molecule stays in an excited singlet state before deexcitation. Absorption, or CD, is a process that is over in 10^{-15} sec. On this time scale, the molecule and its environment are effectively static.

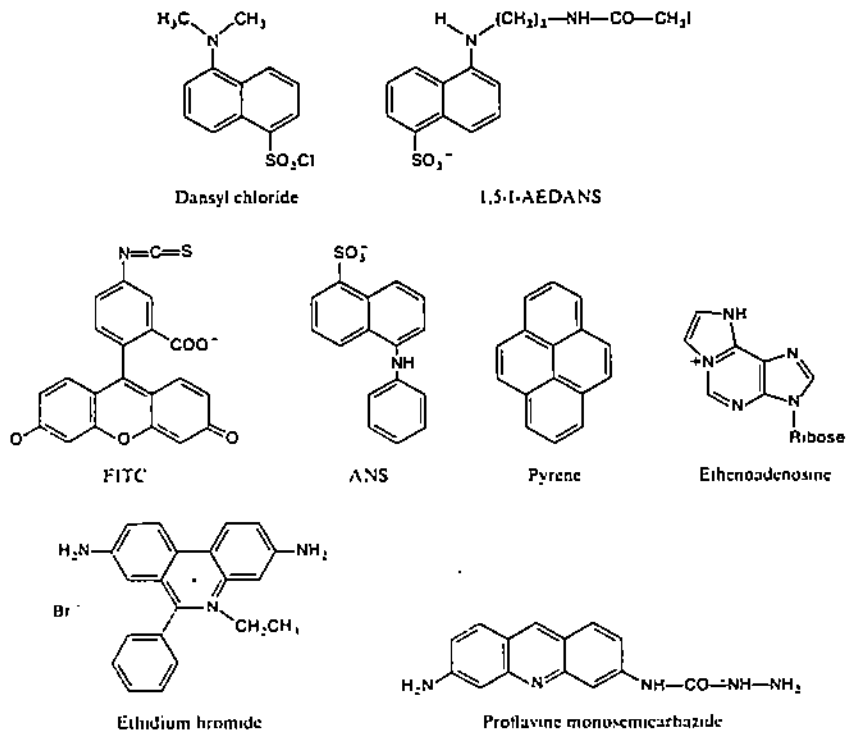

Figure 8-16

Structures of fluorescent probes listed in Table 8-3.

In contrast, during the 10^{-9} to 10^{-8} sec that a singlet remains excited, all kinds of processes can occur, including protonation or deprotonation reactions, solvent-cage relaxation, local conformational changes, and any processes coupled to translational or rotational motion.

A number of fluorescent molecules have a very convenient property: in aqueous solution their fluorescence is very strongly quenched, but in a nonpolar or a rigid environment a striking enhancement is observed. This enhancement can easily be by more than a factor of 20. If the probe can bind to a rigid or nonpolar site on a protein or nucleic acid, the fluorescence spectrum will be dominated by the bound species. Figure 8-17 shows a typical example.

For proteins, the dye 8-anilinonaphthalene sulfonate (ANS) is the most frequently used environmental probe, although several other common ones exist. Ethidium is

Table 8-3
Typical fluorescent probes

Probe[a]	Uses	Absorption		Emission[a]			Sensitivity
		λ_{max} (nm)	$\epsilon_{max} \times 10^{-3}$	λ_{max} (nm)	ϕ_f	τ_f (nsec)	$\epsilon_{max}\phi_f \times 10^{-3}$
Dansyl chloride	Covalent attachment to protein: Lys, Cys	330	3.4	510	0.1	13	3.4
1,5-I-AEDANS	Covalent attachment to protein: Lys, Cys	360	6.8	480	0.5	15	34
Fluorescein isothiocyanate (FITC)	Covalent attachment to protein: Lys	495	42	516	0.3	4	116
8-Anilino-1-naphthalene sulfonate (ANS)	Noncovalent binding to proteins	374	6.8	454	0.98	16	67
Pyrene, and various derivatives	Polarization studies on large systems	342	40	383	0.25	100	100
Ethenoadenosine, and various derivatives	Analogs of nucleotides bind to proteins, incorporate into nucleic acids	300	2.6	410	0.40	26	10
Ethidium bromide	Noncovalent binding to nucleic acids	315	3.8	600	~1	26.5	38
Proflavine monosemiurbromide	Covalent attachment to RNA 3′-ends	445	15	516	0.02		30

[a] Values shown for ϕ_f and τ_f are near the maximum typically observed in biological samples at ambient temperature. Other (considerably smaller) values often are found.
[b] Structures of these probes are shown in Figure 8-16.

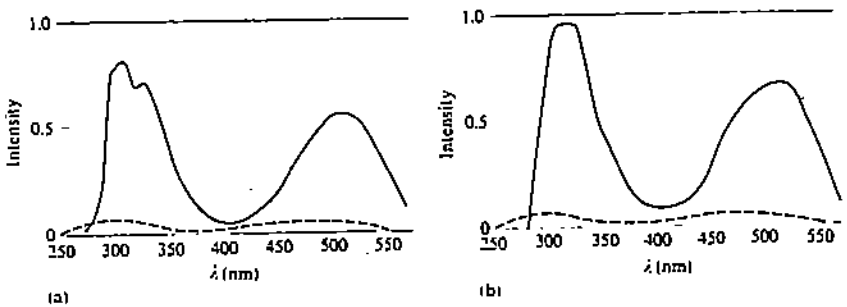

Figure 8-17
Fluorescence excitation spectra of ethidium bromide in aqueous solution (*dashed line*) or bound (*solid line*) to (a) double-strand DNA or (b) RNA. Emission is monitored at 6.00 nm. [After a figure provided by J. B. LePecq and J. Paoletti.]

most often used for nucleic acids. Ethidium in aqueous solution has very weak fluorescence but, when it intercalates into double-helical regions of a nucleic acid, the fluorescence is very intense. For a fixed total concentration of a fluorescence probe, changes in the number or strengths of binding sites will lead to large alterations in the observed fluorescence. This property obviously can permit accurate measurements of variety of interesting phenomena.

Another environmental effect is the accessibility of a fluorescent chromophore to collisional quenching by solute molecules. Oxygen is a ground-state triplet. Collision with an excited singlet leads to an enhanced rate of singlet–triplet interconversion (intersystem crossing) and thus to quenching of the fluorescence. Any heavy atom (such as iodide or cesium ions) has a similar effect, although the fundamental mechanism is different. A chromophore free in aqueous solution is quite susceptible to such quenching. When incorporated into a macromolecular structure, it may be considerably shielded from the solvent. This shielding can show up as a protection against quenching. Fluorescence, measured as a function of quencher concentration, often can help to discriminate residues on the surface of a protein from those deeply buried. Sometimes these differences are masked by complex effects of the local environment. For example, anionic groups near a chromophore may make it difficult for negatively charged ions such as I^- to approach close enough to quench.

To analyze the effect of a quencher, start with Equations 8-35 and 8-36. If the fluorescence in the presence (F) and in the absence (F_0) of the quencher (or the corresponding quantum yields, ϕ and ϕ_0) are compared, at constant concentration and sample geometry, we have

$$\begin{aligned} F_0/F = \phi_0/\phi &= [k_F + k_{ic} + k_{is} + k_q(Q)]/(k_F + k_{ic} + k_{is}) \\ &= 1 + k_q\tau_0(Q) \end{aligned} \tag{8-46}$$

where τ_0 is the lifetime in the absence of quencher: $\tau_0 = (k_F + k_{ic} + k_{is})^{-1}$. Because τ_0 can be measured, a plot of F_0/F versus (Q) should yield k_q. Table 8-4 shows some typical values of bimolecular quenching constants. The quenching constant for a free chromophore is of the order of 10^{10} M^{-1} sec^{-1}. Such a rapid rate is characteristic of a diffusion-controlled reaction. However, when chromophores are bound to or incorporated into proteins, k_q sometimes is substantially smaller.

Table 8-4
Quenching of tryptophan fluorescence by collision with small molecules

Protein	Native protein (0.1 M phosphate, pH 7) $k_q \times 10^{-9}$ M^{-1} sec^{-1}		Denatured protein (6 M guanidine·HCl added) $k_q \times 10^{-9}$ M^{-1} sec^{-1}	
	Oxygen	Iodide	Oxygen	Iodide
Tryptophan	12.0	3.9	5.9	1.9
n-Ac-Try-NH_2	11.6	3.8	7.3	2.1
Pepsin	5.7	1.7	4.3	1.8
Trypsinogen	4.3	0.3	6.1	1.2
Carboxypeptidase A	3.8	0.3	5.8	1.1
Carbonic anhydrase	2.6	0.2	4.2	1.0

SOURCE: Adapted from J. R. Lakowicz and G. Weber, *Biochemistry* 12:4171 (1973).

Singlet–singlet energy transfer

A fairly unique feature of fluorescence is the ability of other chromophores quite far away from an excited singlet to cause quenching. In a favorable case, this permits distances between chromophores to be measured up to a range of about 80 Å. Consider a system with just one copy each of two different chromophores, with individual spectra as shown in Figure 8-18. If these chromophores are within a few angstroms, they can interact by the exciton (coupled oscillator) mechanism as described earlier. In this case, splittings and shifts in the apparent locations of spectral bands can occur. This is not the case we want to consider here.

Optical interactions persist between the two chromophores even when they are so far apart that no changes in the shapes of their spectra are observed. This is called the very weak coupling limit. It is convenient to define the component with higher energy absorption as the donor (D), and the other as the acceptor (A). We consider just the ground singlet states (D_a, A_a) and first excited singlet states (D_b, A_b) of each chromophore. Suppose that the donor is excited. It will rapidly lose energy by internal conversion until it reaches the ground vibrational level of the first excited singlet, D_b. If donor emission energies are coincident with acceptor absorption energies, the very weak coupling can permit the following resonance to take place:

$$D_b + A_a \underset{k_{-T}}{\overset{k_T}{\rightleftharpoons}} D_a + A_b \qquad (8\text{-}47)$$

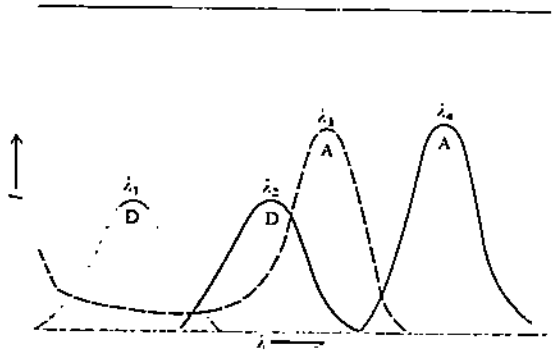

Figure 8-18
Schematic spectra for a donor–acceptor pair suitable for singlet–singlet energy-transfer measurements. Shown are the absorption spectra for donor (*colored line*) and acceptor (*dashed line*), and the emission spectra for donor (*black line*) and acceptor (*gray line*). The spectral overlap (neglecting the factor of ν^{-4}) is shaded.

As shown in Figure 8-19, the resulting acceptor singlet (A_b) and donor singlet (D_a) are in excited vibrational states. Vibrational relaxation rapidly converts these to the ground vibrational level. Therefore, even when k_T is an efficient process, the reverse reaction (k_{-T}) is unlikely to occur. The energy-transfer resonance shifts the relative population of excited donors and acceptors. The donor becomes quenched. The acceptor becomes excited, and subsequently it can fluoresce. This process, from the viewpoint of the acceptor, is called sensitized emission. Note that the two chromophores need not necessarily be part of the same molecule. Energy transfer will take place between isolated molecules in solution as long as the concentration is high enough to bring average intermolecular distance within 50 Å or so.

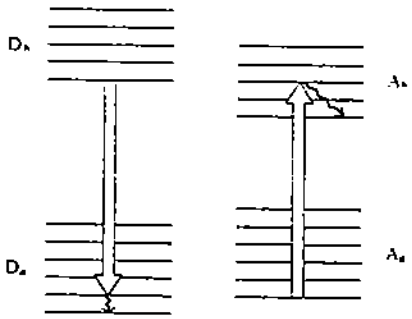

Figure 8-19
Donor deexcitation and acceptor excitation coupled in the resonant interaction that leads to energy transfer. Vibrational relaxation (*wavy arrows*) occurs rapidly and tends to prevent a repeat of the interaction that would relax the acceptor and reexcite the donor.

Singlet–singlet energy transfer can be observed in several ways. Define the efficiency of transfer (E) as the fraction of D_b that is deexcited by transfer to the acceptor:

$$E = k_T/(k_T + k_F^D + k_{ic}^D + k_{is}^D) \tag{8-48}$$

where k_T is the rate of energy transfer, and all other rates refer to donor processes. In Figure 8-18, if the system is excited at λ_1 and observed at λ_2, only emission from D is seen. Two samples must be prepared as identical as possible, except that one contains both donor and acceptor, whereas the other has only donor. When the fluorescence of these two samples is compared, E can be measured. Using Equations 8-36 and 8-48, it is easy to show that

$$\phi_{D+A}/\phi_D = [k_F^D/(k_F^D + k_{ic}^D + k_{is}^D + k_T)] \times [(k_F^D + k_{ic}^D + k_{is}^D)/k_F^D] = 1 - E \tag{8-49}$$

where ϕ_{D+A} is the quantum yield of the donor in the presence of the acceptor.

An alternative experimental arrangement involves keeping the emission wavelength constant at λ_4 and varying the excitation wavelength from λ_3 to λ_1. If the system contains only acceptor, the excitation will just resemble its absorption. But, if donor is present also, there will be an additional peak in the excitation spectrum, corresponding to the absorption maximum of the donor at λ_1. The intensity of this peak will depend on the relative absorbance of donor and acceptor in the region of λ_1, and on the efficiency of transfer (E). At λ_4, only acceptor fluorescence can be observed. For constant experimental geometry and incident light, we can use Equation 8-42 to analyze the result. The relative fluorescence of the sample with acceptor alone (exciting at λ_1 and observing at λ_4) will be

$$F_A \propto \varepsilon_A C_A \phi_A \tag{8-50}$$

whereas the sample with both donor and acceptor will have more fluorescence:

$$F_{D+A} \propto \varepsilon_A C_A \phi_A + \varepsilon_D C_D E \phi_A \tag{8-51}$$

In Equation 8-51, $\varepsilon_D C_D$ is proportional to the number of excited donors: E is the fraction of the excited donors that transfer energy, resulting in an excited acceptor. Combining the results of these two measurements, one can determine E:

$$F_{D+A}/F_A = 1 + (\varepsilon_D C_D/\varepsilon_A C_A)E \tag{8-52}$$

A third independent measurement of E can be obtained by comparing the fluorescence decay times of the donor in the presence ($\tau_{D,A}$) and absence (τ_D) of the acceptor. You should be able to show that

$$\tau_{D,A}/\tau_D = 1 - E \tag{8-53}$$

Measurement of energy transfer by direct observation of lifetimes is quite important because it avoids a potential trivial effect that can mimic transfer.

A requirement for the resonance interaction producing energy transfer is that acceptor absorption must overlap the donor fluorescence (Fig. 8-18). Therefore, in any system capable of energy transfer, an additional process may occur in which the donor emits a photon that is then reabsorbed by the acceptor. This is distinguishable from true singlet–singlet energy transfer, because it leaves the rate of donor emission unchanged. Trivial emission and reabsorption of photons can be detected by comparing the efficiencies derived from Equations 8-53 and 8-49 or 8-52. It can be avoided by working at total chromophore concentrations less than about 10^{-3} M.

Measuring interchromophore distances from energy-transfer efficiencies

To obtain useful structural information from energy transfer, the measured efficiency must be related to the distance R between the two chromophores. This can be done by using the theory developed by Theodore Förster. He computed that the rate of transfer is

$$k_T = (1/\tau_D)(R_0/R)^6 \tag{8-54}$$

where τ_D is the lifetime of the donor in the absence of the acceptor. The inverse sixth power comes from the square of the dipole–dipole coupling, which depends on R^{-3} (see Box 8-3). R_0 is called the characteristic transfer distance:

$$R_0 = 9.7 \times 10^3 (J\kappa^2 n^{-4} \phi_D)^{1/6} \text{ cm} \tag{8-55}$$

where

$$J = \int \varepsilon_A(\nu) f_D(\nu) \nu^{-4} \, d\nu \tag{8-56}$$

J is a measure of the spectral overlap between donor emission and acceptor absorption (shaded in Fig. 8-18); f_D is the normalized fluorescence of the donor as defined in Equation 8-42; n is the refractive index of the medium between donor and acceptor; ϕ_D is the quantum yield of donor in the absence of the acceptor; and κ^2 is a complex geometric factor that depends on the orientation of donor and acceptor. If both donor and acceptor are free to tumble rapidly on the time scale of fluorescence emission, κ^2 approaches a limiting value of 2/3. (The origins of all these quantities in Eqns. 8-54, 8-55, and 8-56 are described in Box 8-3.)

Box 8-3 THE FÖRSTER THEORY OF SINGLET–SINGLET ENERGY TRANSFER

Here we sketch an oversimplified derivation of Equations 8-54, 8-55, and 8-56. We start with Equation 7-27, which says that the rate of exciting a molecule is proportional to the square of the expectation value of the interaction causing the excitation. Although we derived this equation for a particular case, it turns out to be a very general result, often called Fermi's Golden Rule. We want to compute the rate at which the state of the chromophore pair D and A changes from $\Psi_{D_a}\Psi_{A_a}$ to $\Psi_{D_a}\Psi_{A_b}$.

We first consider the case where the $a \rightarrow b$ transitions of both D and A occur at the same frequency, ν. To describe the weak interaction between D and A, we use the same dipole–dipole coupling described earlier for the somewhat stronger interactions that produce exciton splitting. Therefore, the rate of energy transfer should be proportional to the following expression:

$$k_T(\nu) \propto |\langle \Psi_{D_a}\Psi_{A_b}|\underline{V}|\Psi_{D_b}\Psi_{A_a}\rangle|^2$$

where $\underline{V}$ is given (by analogy to Eqn. 7-48) as

$$\underline{V} = (\underline{\mu}_D \cdot \underline{\mu}_A)/R^3 - 3(\underline{\mu}_D \cdot \mathbf{R})(\mathbf{R} \cdot \underline{\mu}_A)\,R^5$$

where $\mathbf{R}$ is the distance between donor and acceptor, and $\underline{\mu}_D$ and $\underline{\mu}_A$ are dipole moment operators.

If all effects of the orientation of D and A are lumped into a parameter κ, then we can rewrite $\underline{V}$ as

$$\underline{V} = \kappa|\underline{\mu}_D||\underline{\mu}_A|\,R^3$$

where the vertical bars indicate that only the lengths of $\underline{\mu}_D$ and $\underline{\mu}_A$ must be evaluated. Substitution of this expression for $\underline{V}$ into the earlier equation for the transfer rate, k_T, yields

$$k_T(\nu) \propto [\kappa^2 R^6]|\langle \Psi_{D_a}\Psi_{A_b}|\underline{\mu}_D|\underline{\mu}_A|\Psi_{D_b}\Psi_{A_a}\rangle|^2$$

Because $\underline{\mu}_D$ depends only on the electronic coordinates of the donor group, and $\underline{\mu}_A$ depends only on the acceptor group, this expression can be factored to give

$$k_T(\nu) \propto (\kappa^2\ R^6)|\langle \Psi_{D_a}^{*}|\underline{\mu}_D|\Psi_{D_b}\rangle|^2|\langle \Psi_{A_b}|\underline{\mu}_A|\Psi_{A_a}\rangle|^2$$

You can see that the transfer rate will depend on the inverse sixth power of the distance. The term in $\underline{\mu}_A$ is just the dipole strength of the acceptor, which in turn can be related to an integral over the absorption spectrum using Equation 7-40. In the case we are considering, absorption takes place only at a single frequency ν, and so Equation 7-40 becomes

$$|\langle \Psi_{A_b}|\underline{\mu}_A|\Psi_{A_a}\rangle|^2 \propto \varepsilon_A\nu^{-1}$$

The term in $\underline{\mu}_D$ is the dipole strength of the donor, which can be related to the fluorescence rate.

Using Equations 8-32 and 8-34, we have

$$D_{ab} \propto \nu^{-3}A_{b_a} = \nu^{-3}\tau_R^{-1}$$

From Equation 8-41, we can replace τ_R^{-1} by ϕ_D/τ_D, where ϕ_D is the quantum yield of the donor, and τ_D is the lifetime of the donor in the absence of the acceptor. Then

$$|\langle \Psi_{D_b}|\underline{\mu}_D|\Psi_{D_a}\rangle|^2 \propto \nu^{-3}\phi_D\,\tau_D$$

Using all these results, we can write the energy transfer rate as

$$k_T(\nu) \propto (\kappa^2\ R^6)[\phi_D\ \tau_D]\varepsilon_A\nu^{-4}$$

Now we consider the general case where the acceptor absorption occurs over a band of frequencies, so that ε_A is a function of ν. Similarly, the fluorescence of the donor occurs over a range of frequencies. Let $f_D(\nu)$ be the fraction of donor fluorescence at frequency ν. The total rate of energy transfer can be computed by integrating the rate expected at each frequency:

$$k_T \propto (\kappa^2\ R^6)[\phi_D\tau_D]\int \varepsilon_A(\nu)f_D(\nu)\nu^{-4}d\nu = (\kappa^2\phi_D R^6\tau_D)J$$

This expression is identical to Equations 8-54, 8-55, and 8-56, except for numerical constants and the appearance of n, the refractive index. The presence of n comes from the fact that $\underline{V}$ as written above applies only in vacuum: in a fluid medium, the true interaction potential at optical frequencies is $\underline{V}\ n^2$.

The troublesome part of the Förster theory is the inclusion of the quantity κ^2. Removing the orientation dependence of the donor and acceptor interaction (as we did above) implies that orientations are sampled rapidly during the time the donor is excited. This may not always be true. Unfortunately, κ^2 cannot be measured directly. From the definition of $\underline{V}$, we know that κ^2 must have a value between 0 and 4. Measurements of fluorescence polarization can place narrower limits on κ^2 in each particular case. Uncertainties in the κ^2 value still are a major source of error in distance determinations using energy transfer. Fortunately, the distance R will depend only on $(\kappa^2)^{1/6}$, as you can see by rewriting Equation 8-57 in this form:

$$R = R_0[(1 - E)/E]^{1/6}$$

In actuality, using Equations 8-55 and 8-56, it is more convenient to use spectra measured on a wavelength scale and to express the result in angstroms. Then Equations 8-55 and 8-56 become

$$R_0 = 8.79 \times 10^{-5}[J\kappa^2 n^{-4}\phi_D]^{1/6}\ \text{Å}$$

$$J = \int \varepsilon_A(\lambda)f_D(\lambda)\lambda^4 d\lambda$$

The efficiency of energy transfer can be calculated by rewriting Equation 8-48 as $E = k_T/(k_T + 1/\tau_D)$. Then, substitution of Equation 8-54 for k_T yields

$$E = R_0^6/(R_0^6 + R^6) \tag{8-57}$$

The result is plotted as the solid line in Figure 8-20 for a particular value of R_0. It is apparent that, for distances near R_0, a measurement of E can yield a fairly accurate determination of the distance. For commonly used pairs of chromophores, R_0 varies from 10 Å to more than 50 Å. Therefore, distances up to about 80 Å are measurable.

The most critical test of the Förster theory came from the work of Lubert Stryer and Richard Haugland (1967). They prepared a set of terminally labeled oligopeptides:

Dansyl—(Pro)$_n$—NH—NH—CO—NH—Naphthyl

The proline residues formed a polyproline type-II helix, which could be confirmed by CD measurements. Because the distance between naphthyl donor and dansyl acceptor was known from the known dimensions of the helix, measured efficiencies could be compared directly with computed values from the Förster theory: the agreement is excellent (Fig. 8-20). Since this pioneering work, energy transfer has been used to measure distances within tRNA, immunoglobulins, rhodopsin, and oligopeptides, and between the protein subunits of assemblies ranging from simple oligomeric proteins to ribosomes. The most difficult part of these measurements is the specific introduction of the two fluorescent chromophores into known portions of the structures. For the full spectrum of measurements, three replica systems must be prepared. They should be as identical as possible, except that one has only donor, one has donor and acceptor, and one has only acceptor.

Energy transfer plays a large role in determining the emission spectrum of normal proteins. The fluorescence of tyrosine is overlapped by the absorption of tryptophan. Although the R_0 for this donor-acceptor pair is only ~9 Å, it is still appreciable compared with average distances expected for tyrosine-tryptophan nearest-neighbor pairs in a globular protein.[1] The result is that the tyrosines are extensively quenched; almost all of the observed emission comes from tryptophan (as we mentioned earlier).

Fluorescence polarization

If plane-polarized light is used to excite a fluorescent system, and if linearly polarized components of the emission are detected, information can be obtained about the size, shape and flexibility of macromolecules. Figure 8-21 shows a typical experimental

[1] A spherical protein of 17,000 mol wt will have a radius (r) of about 17 Å. The root-mean-square distance between random selected pairs of points within a spherical volume is $\sqrt{6/5}\,r$. So even a single tryptophan in such a protein is likely to be near enough to many tyrosines to cause appreciable energy transfer.

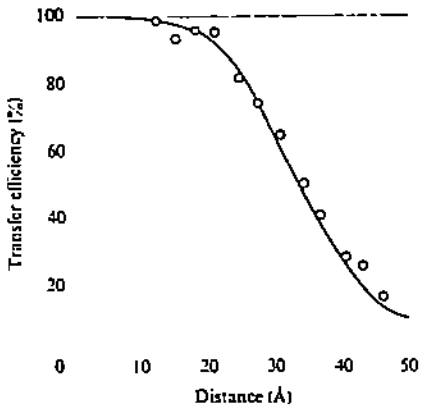

Figure 8-20
Efficiency of energy transfer as a function of distance in dansyl-(L-prolyl)$_n$-α-naphthyl semicarbazide oligomers with $n = 1$ to 12. The curve was fit to the data with Equation 8-57. [From L. Stryer and R. P. Haugland, *Proc. Natl. Acad. Sci. USA* 58:719 (1967).]

arrangement. Light is incident along the x axis and is detected along the y axis. The incident light is polarized along the z axis. Two components of the emitted light are measured: $I_{\parallel}$ is polarized along the z axis, and $I_{\perp}$ is polarized along the x axis. There can be no emission propagating along the y axis that is also polarized along this axis because light, like all electromagnetic radiation, is a transverse wave.

Polarization of rigid systems

First, consider a rigid, isotropic sample. This sample could correspond to a frozen solution of fluorescent molecules, or to chromophores on randomly oriented molecules so large that no appreciable molecular rotations occur on the fluorescence time scale (typically < 100 nsec). The vector $\boldsymbol{\mu}$ defines the orientation of the absorption transition dipole moment ($\langle \Psi_b|\boldsymbol{\mu}|\Psi_a\rangle$) of one chromophore relative to the laboratory coordinates. The probability that this chromophore will be excited is proportional to $(\boldsymbol{\mu} \cdot \mathbf{E})^2$. Because $\mathbf{E}$ is parallel to the z axis, this probability is $\cos^2\theta$, where θ is the angle between $\boldsymbol{\mu}$ and the z axis. Therefore, molecules oriented with transition dipoles near the z axis will be preferentially excited. This is the principle called *photoselection*.

To explain fluorescence polarization, we need to calculate the probability of exciting molecules with particular orientations. Then we must compute the probability that these molecules will emit light polarized in certain directions. It is convenient to use spherical polar coordinates (Fig. 8-21). Before excitation, the relative number of molecules with μ oriented at angles between θ to $\theta + d\theta$ and ϕ to $\phi + d\phi$ is $\sin\theta\, d\theta\, d\phi$. (The factor of $\sin\theta$ enters because it is much more probable to find molecules perpendicular to the z axis than parallel to it.) The probability of exciting a molecule oriented at θ and ϕ is proportional to $\cos^2\theta$, as mentioned earlier. Therefore, the

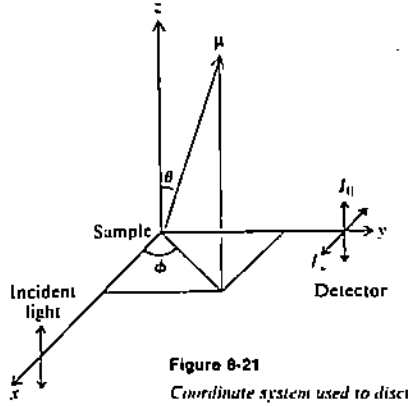

Figure 8-21
Coordinate system used to discuss fluorescence polarization.

relative number of excited molecules oriented at θ to $\theta + d\theta$ and ϕ to $\phi + d\phi$ is

$$P(\theta, \phi)\, d\theta\, d\phi \propto \cos^2\theta \sin\theta\, d\theta\, d\phi \tag{8-58}$$

The fraction of excited molecules oriented at θ to $\theta + d\theta$ and ϕ to $\phi + d\phi$ is

$$W(\theta, \phi)\, d\theta\, d\phi = P(\theta, \phi)\, d\theta\, d\phi \Big/ \int_0^{\pi} d\theta \int_0^{2\pi} d\phi \cos^2\theta \sin\theta\, d\theta\, d\phi \tag{8-59}$$

The integral in Equation 8-59 simply counts all excited molecules. It can be performed by substituting $x = \cos\theta$, $dx = -\sin\theta$, and so on. The result is $4\pi/3$, so Equation 8-59 becomes

$$W(\theta, \phi)\, d\theta\, d\phi = (3/4\pi) \cos^2\theta \sin\theta\, d\theta\, d\phi \tag{8-60}$$

Note that this result depends only on θ. The distribution of excited molecules is cylindrically symmetric about the z axis. (Fig. 8-22 shows a plot of Eqn. 8-60.) Note that excited molecules have transition dipoles oriented preferentially toward the z axis and not along the x axis.

Because the distribution of excited molecules is anisotropic, the resulting fluorescence also will be anisotropic. To calculate this, we must know the relative directions of absorbing and emitting transition dipoles in the chromophore. If the same electronic transition that absorbed does the emitting ($S_a \rightarrow S_b$ followed by $S_b \rightarrow S_a$), then emitting and absorbing transition dipoles are parallel. The probability that emission will occur polarized along the z axis is proportional to $|\boldsymbol{\mu} \cdot \hat{\mathbf{k}}|^2$, where $\hat{\mathbf{k}}$ is a unit vector along the z axis. This expression is proportional to $\cos^2\theta$. To find the relative emission intensity polarized along z, we must multiply the probability

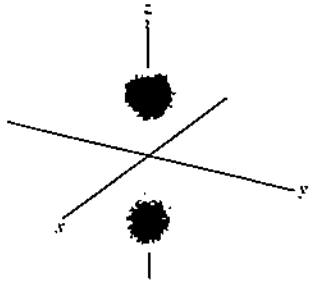

Figure 8-22
Distribution of excited chromophores produced by exciting a sample with z-polarized light propagating along the x axis. The density of the shading is proportional to the probability of finding an excited molecule with its transition dipole at that particular orientation.

of emission by the fraction of excited molecules with each orientation, $W(\theta, \phi)$, and average over all orientations:

$$I_{\parallel} \propto \int_0^{2\pi} d\phi \int_0^{\pi} d\theta \cos^2\theta\, W(\theta, \phi) = (3/4)\pi \int_0^{2\pi} d\phi \int_0^{\pi} d\theta \cos^4\theta \sin\theta = 3/5 \tag{8-61}$$

The probability of emission polarized along the x axis is proportional to $|\boldsymbol{\mu} \cdot \hat{\mathbf{i}}|^2$, where $\hat{\mathbf{i}}$ is a unit vector along x. This expression is proportional to $(\sin\theta \cos\phi)^2$. To calculate the relative emission intensity, $I_{\perp}$, we again average emission probabilities over the distribution of excited molecules:

$$I_{\perp} \propto \int_0^{2\pi} d\phi \int_0^{\pi} d\theta \sin^2\theta \cos^2\phi\, W(\theta, \phi) = (3/4)\pi \int_0^{2\pi} d\phi \cos^2\phi \int_0^{\pi} d\theta \cos^2\theta \sin^3\theta = 1/5 \tag{8-62}$$

In practice, what is done is to measure $I_{\parallel}$ and $I_{\perp}$ and compare. Two convenient comparisons of $I_{\parallel}$ and $I_{\perp}$—the polarization (P) and the anisotropy (A)—are defined in Equation 8-63 (see also Box 8-4).

$$P = (I_{\parallel} - I_{\perp})/(I_{\parallel} + I_{\perp}) \qquad A = (I_{\parallel} - I_{\perp})/(I_{\parallel} + 2I_{\perp}) \tag{8-63}$$

For the totally rigid system we have just described, $P = 1/2$ and $A = 2/5$, as you can see by substituting the results of Equations 8-61 and 8-62 into Equation 8-63. These turn out to be the maximal values of polarization and anisotropy possible under any circumstances.

Box 8-4 POLARIZATION AND ANISOTROPY

The definitions of polarization and anisotropy are not as arbitrary as they seem. P is defined by analogy with the dichroic ratio described in Equation 7-42. It is a relatively simple quantity to measure directly. A is more useful for analysis of experimental data on complex systems. The denominator of A is simply the total light that would be observed if no polarizers were used (see figure). Nonpolarized light incident along x can be resolved into y- and z-polarized

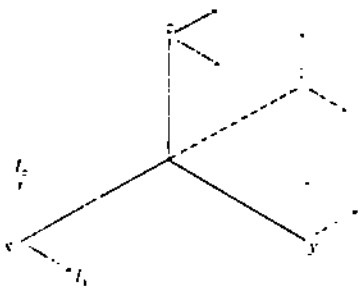

components. The total emission can be found by adding emission along all three Cartesian axes. For z-polarized excitation, there are two perpendicular components propagating along z, and one parallel and one perpendicular component, each propagating along x and y. For y-polarized excitation, there are two perpendicular components propagating along y, and one parallel and one perpendicular component, each propagating along x and z. The result is $4I_\perp$ plus $4I_\parallel$. Therefore, the total emission has twice as much perpendicular component as parallel component.

Anisotropy has a substantial advantage in many applications because various equations using it are simpler than the corresponding equations for polarization. Another advantage comes in the analysis of mixtures. Multicomponent mixtures of substances with equal fluorescence intensity but variable anisotropy (A_i) show a total anisotropy equal to $\sum_i \chi_i A_i$, where χ_i is the mole fraction of the ith component. Polarization does not obey such simple relationships. However, polarization and anisotropy can be interconverted by the relationship

$$[(1/P) - (1/3)]^{-1} = 3A/2$$

which you should be able to derive from Equation 8-63.

Another common case is a system in which the emission transition dipole is perpendicular to the absorption transition dipole. This will occur in many planar chromophores if absorption takes place into the second excited singlet state, but emission is observed from the first excited singlet. In this case, still for a rigid system, $P = -1/3$ and $A = -1/5$. See if you can derive these values by calculating averages analogous to those worked out for the case just discussed.

The polarization or anisotropy for a rigid system is called the limiting value, and it is denoted by subscript zero. In general, it is given by

$$P_0 = (3\cos^2\xi - 1)/(\cos^2\xi + 3) \qquad A_0 = (3\cos^2\xi - 1)/5 \tag{8-64}$$

where ξ is the angle between absorption and emission transition dipoles. These expressions provide a method of measuring ξ in rigid systems.

Now consider the other extreme case, in which (during the lifetime of the excited state) the chromophore can tumble fast enough to randomize its orientation. In this case, by the time emission occurs, all memory of the original photoselection is lost. Thus $I_\parallel = I_\perp$, and the polarization and anisotropy are both zero.

• Effect of molecular motion

Most macromolecules of biological interest fall between the two extreme cases just described: their rotational motions are *not* negligible on the fluorescence time scale, but neither can they tumble fast enough to achieve random orientation. Suppose that a fluorescent probe is rigidly attached to the macromolecule. The observed polarization will be some intermediate value between Equation 8-64 and zero. To compute this value, we must analyze the relative rates of emission and macromolecular rotational motion. Note that translational motion does not affect fluorescence polarization. Only motion that changes the *orientation* of the transition dipoles can be observed.

First consider what happens if the sample is excited by a pulse of polarized light, and the time dependence of $I_\parallel$ and $I_\perp$ is measured. If emission and absorption dipoles are parallel, the earliest photons to be emitted are highly likely to be z-polarized because the molecules have not had time to reorient. The last photons to be emitted should have random polarization because by then the system has experienced considerable rotational motion. Therefore, if the polarization or anistropy is measured as a function of the time of fluorescence emission, it will decay from initial values of P_0 or A_0 to final values of zero. The rate of decay is a measure of the rate of rotational motion.

Rotational Brownian motion is described by a diffusion equation quite analogous

to that used for translational motion.[1] If $W(\theta, \phi, t)$ is the probability per unit interval of θ and ϕ that a spherical molecule has orientation θ, ϕ at time t, then

$$dW(\theta, \phi, t)/dt = D_{rot} \nabla^2 W(\theta, \phi, t) \tag{8-65}$$

D_{rot} (the rotational diffusion coefficient) is related to the rotational friction coefficient (f_{rot}):

$$D_{rot} = kT/f_{rot} = kT/6V_h\eta \tag{8-66}$$

where V_h is the hydrated volume of the molecule, T is the absolute temperature, and η is the viscosity of the solution.

$W(\theta, \phi, t)$ gives the probability that any molecule has a particular orientation at time t. However, in polarization measurements, we observe only those molecules initially excited at time zero. From Equation 8-60, we can write the initial distribution of excited molecules as

$$W(\theta, \phi, 0) = (3/4\pi) \cos^2 \theta \sin \theta \tag{8-67}$$

Solving Equation 8-65 using this boundary condition yields an explicit expression for $W(\theta, \phi, t)$. This expression is a function of the rotational diffusion coefficient just defined. It tells the angular distribution of absorption transition dipoles at any time t.

The population of excited singlets produced at time zero decays with time according to Equation 8-39. Therefore, we must correct $W(\theta, \phi, t)$ to compute the distribution of molecules that are still excited at time t. This expression is

$$W(\theta, \phi, t)e^{-t/\tau_F} \tag{8-68}$$

If emitting and absorbing dipoles are parallel, then the possibility that a photon emitted from an excited molecule oriented at θ, ϕ is polarized along the x or y direction (P_x or P_y) is proportional to $\cos^2 \theta$ or $\sin^2 \theta \cos^2 \phi$, as discussed earlier. In the more general case, the probability of emission along a particular axis is also a function of the angle ξ between absorption and emission dipoles. We can write this as $P_a(\theta, \phi, \xi)$, where the subscript a refers to the axis of the polarized component emitted.

If we now combine $P_a(\theta, \phi, \xi)$ and $W(\theta, \phi, t)e^{-t/\tau_F}$, we have the probability that a molecule excited at time zero will emit a photon at time t polarized along a. Integrating this probability over all orientations gives the expected intensity of polarized emission along a particular axis as a function of time:

$$I_a(t) = \int_0^{2\pi} d\phi \int_0^{\pi} d\theta \, P_a(\theta, \phi, \xi) W(\theta, \phi, t) e^{-t/\tau_F} \tag{8-69}$$

[1] The reader who has had little prior experience with diffusion equations is encouraged to read Sections 10-3 and 12-2 for a justification of the form of Equation 8-65 and a demonstration of some of its properties.

This integral can be evaluated using explicit forms for P_a and W. The results for parallel and perpendicular polarization directions are the following:

$$I_{\parallel}(t) = [(1/3) + (4/15)e^{-6D_{rot}t}(3 \cos^2 \xi - 1)/2]e^{-t/\tau_F} \tag{8-70}$$

$$I_{\perp}(t) = [(1/3) - (2/15)e^{-6D_{rot}t}(3 \cos^2 \xi - 1)/2]e^{-t/\tau_F} \tag{8-71}$$

Thus, although the decay of nonpolarized emission is a single exponential, each of the polarized components decays as the sum of two exponentials. If Equations 8-70 and 8-71 are substituted into the definition of fluorescence anisotropy, $A(t)$, the result is particularly simple:

$$A(t) = [I_{\parallel}(t) - I_{\perp}(t)]/[I_{\parallel}(t) + 2I_{\perp}(t)] = (2/5)e^{-6D_{rot}t}[(3 \cos^2 \xi - 1)/2] \tag{8-72}$$

We define the rotational correlation time τ_c as

$$\tau_c = 1.6D_{rot} = V_h\eta/kT \tag{8-73}$$

Then

$$A(t) = (2/5)e^{-t/\tau_c}[(3 \cos^2 \xi - 1)/2]$$

Note that, in the limit of $t \to 0$, Equation 8-72 simplifies to Equation 8-64.

Thus, the decay of the fluorescence anisotropy of a spherical molecule is a single exponential. A measurement of the decay constant τ_c permits the hydrated molecular volume (V_h) to be calculated if the viscosity is known. Equation 8-73 indicates that the larger the molecule, the slower the decay of the fluorescence anisotropy. This is a reasonable result because larger molecules rotate more slowly. Figure 8-23 shows an example of anisotropy decay data for anthraniloyl chymotrypsin. The measured rotational correlation time is 15 nsec. This is a typical value for a small protein.

If the molecular weight and partial specific volume are known, Equation 10-10 can be used to estimate V_h. The hydrated specific volume of a typical protein is about 1 cm^3 g^{-1}. Therefore, the hydrated volume of a single molecule will be $M/N_0 = (M/6) \times 10^{-23}$ cm^3. The value of η for water at 20°C is about 0.01 centipoise; T is 293 K; k is 1.38×10^{-16} erg deg^{-1}. Thus τ_c can be estimated from Equation 8-73 as

$$\tau_c = (0.01 \times M \times 10^{-23})/(6 \times 293 \times 1.38 \times 10^{-16}) = (M/2.4) \times 10^{-12} \text{ sec} \tag{8-74}$$

Roughly, τ_c is 1 nsec for each 2,400 daltons of protein molecular weight, if the protein is approximately spherical. (Equation 8-74 is also approximately correct for globular nucleic acids.) For the example shown in Figure 8-23, the molecular weight is 25,000 daltons; thus τ_c is predicted to be 10 nsec. The difference between predicted and experimental rates arises because chymotrypsin is not a sphere. Elongated shapes rotate more slowly (see Chapter 10).

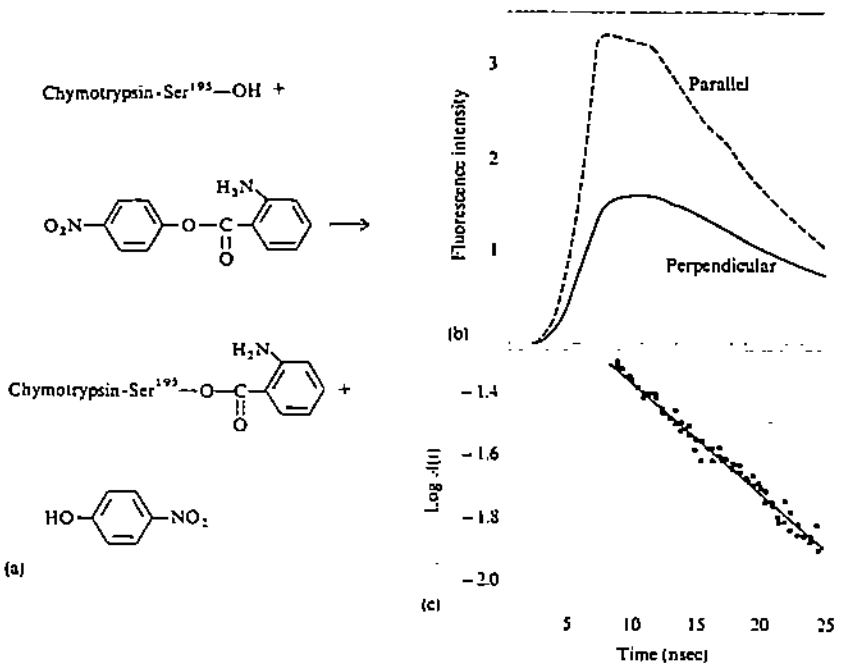

Figure 8-23

Decay of fluorescence anisotropy of anthraniloyl-Ser^{195}-α-chymotrypsin. (a) Preparation of this derivative. (b) Fluorescence decay data for individual polarized components. (c) The anisotropy on a logarithmic scale after deconvolution of the data in order to remove any effects of the shape of the exciting pulse. [After L. Stryer, *Science* 162:526 (1968).]

More often than not, what is measured is the average emission polarized parallel or perpendicular, rather than the time decay. For example,

$$\bar{I}_{\parallel} = \tau_F^{-1} \int_0^{\infty} I_{\parallel}(t)\,dt \qquad \bar{I}_{\perp} = \tau_F^{-1} \int_0^{\infty} I_{\perp}(t)\,dt \tag{8-75}$$

These averages values will be observed if constant illumination is employed. Such measurements are called steady-state or static polarization. Equations 8-70 and 8-71 are inserted into Equation 8-75 to compute expected values of the static polarization and anisotropy:

$$\bar{P} = \frac{\bar{I}_{\parallel} - \bar{I}_{\perp}}{\bar{I}_{\parallel} + \bar{I}_{\perp}} = \frac{3}{1 + 10(1 + \tau_F/\tau_c)(3\cos^2\xi - 1)^{-1}} \tag{8-76}$$

$$\bar{A} = \frac{\bar{I}_{\parallel} - \bar{I}_{\perp}}{\bar{I}_{\parallel} + 2\bar{I}_{\perp}} = \frac{3\cos^2\xi - 1}{5(1 + \tau_F/\tau_c)} \tag{8-77}$$

Suppose that measurements are made at such high values of η/T that the macromolecule is unable to rotate during the lifetime of the excited state. In this case, $\tau_F/\tau_c = 0$, and the polarization and anisotropy become

$$\bar{P}_0 = 3/[1 + 10(3\cos^2\bar{\xi} - 1)^{-1}] = (3\cos^2\bar{\xi} - 1)/(\cos^2\bar{\xi} + 3) \tag{8-78}$$

$$\bar{A}_0 = (3\cos^2\bar{\xi} - 1)/5 \tag{8-79}$$

These values, called the limiting polarization and anisotropy, are precisely the same results as those derived in Equation 8-64 for a rigid system.

The Perrin equations and steady-state polarization measurements

Using the limiting values given for Equations 8-78 and 8-79, we can rewrite Equations 8-76 and 8-77 in a particularly convenient form called the Perrin equations:

$$1/\bar{P} - 1/3 = (1/\bar{P}_0 - 1/3)(1 + \tau_F/\tau_c) = (1/\bar{P}_0 - 1/3)(1 + \tau_F kT/V_h\eta) \tag{8-80}$$

$$\bar{A}^{-1} = \bar{A}_0^{-1}(1 + \tau_F/\tau_c) = \bar{A}_0^{-1}(1 + \tau_F kT/V_h\eta) \tag{8-81}$$

On the right-hand side of the Perrin equations, the rotational correlation time (τ_c) has been expressed explicitly using Equation 8-73. Of all the expressions we have written for polarization, these are the ones most often used in practice. The static polarization or anisotropy of a macromolecular solution is measured as a function of temperature T or viscosity η. When the results are plotted according to Equation 8-80 or 8-81, a straight line should result. The slope will yield the molecular volume (V_h), providing that the fluorescence decay time (τ_F) is known. The intercept at $T/\eta \to 0$ will yield the limiting anisotropy or polarization. Figure 8-24 shows an example of such a Perrin plot for chymotrypsin. The limiting anisotropy (0.3) suggests that the fluorescence probe is nearly rigidly attached. The rotational correlation time (15 nsec) agrees with the value obtained from time-dependent measurements. It is reasonably close to what is expected for a rigid spherical protein, as estimated earlier.

All of Equations 8-65 through 8-81 hold only for spherical molecules. If, instead, a rigid ellipsoid is a more accurate description of the system, the results become much

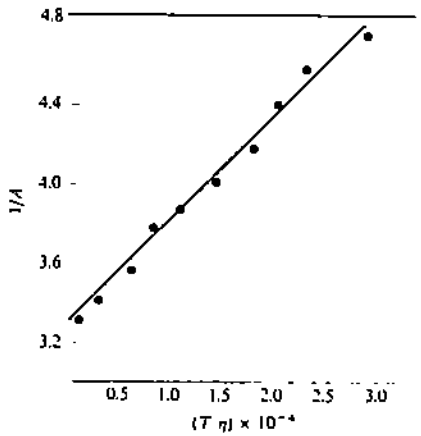

Figure 8-24

Static fluorescence polarization of anthraniloyl-Ser^{195}-α-chymotrypsin (see Fig. 8-23). To generate this Perrin plot, the temperature was maintained constant at 20 C while the viscosity was varied by the addition of glycerol to aqueous solutions of the protein. [After R. P. Haugland and L. Stryer, in *Conformation of Biopolymers*, vol. 1, ed. G. N. Ramachandran (New York: Academic Press, 1967).]

more complicated. The rotational diffusion constant needed for Equation 8-65 now is a tensor. The decay of fluorescence anisotropy, instead of a single exponential as in Equation 8-72, now contains a sum of as many as five exponentials. These exponentials depend not only on the size and shape of the molecules, but also on the orientation of the transition dipoles of the chromophores with respect to the axes of the ellipsoid. In principle, if accurate enough data could be obtained, measurement of anisotropy decay could lead to a detailed picture of the shape of the molecule and the mode of binding of the chromophore. In practice, it is rare that the accuracy of the data justifies fitting to more than two exponentials. In this case, the best one can do is to construct various plausible models for the structure and see how they fit the data. One generalization can be stated: a prolate ellipsoid will tend to have an apparent τ_c larger than that of a sphere. Hence, if the molecular weight is known, some information about axial ratios usually can be obtained.

Suppose that an anisotropy is found to be smaller than that calculated for a spherical molecule of known atomic weight. This is an indication of flexibility of the macromolecule as a whole, or of nonrigid attachment of the chromophore to the macromolecule. Sometimes these effects can be distinguished by carrying out polarization measurements at very high values of T/η. The hydrated volume of a single chromophore is about 1% or less of the volume of a typical macromolecule. If the chromophore is free to move, its rotational correlation time will be about 1/100 that of the macromolecule. At low viscosity, the chromophore will experience all accessible orientations in a period of time that is short compared with the fluorescence lifetime. If these orientations cover a wide range of angles, the observed polarization will be zero. If, however, the rapid motions of the chromophore cover only a limited

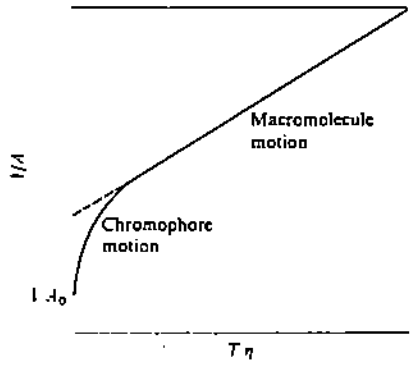

Figure 8-25

Schematic Perrin plot of anisotropy versus temperature or viscosity for a sample in which there is some *limited* flexibility in the attachment of the fluorescent moiety to a macromolecule. Extrapolation of the linear portion to $T\eta = 0$ (*dashed line*) yields an apparent value for A_0 considerably smaller than the true value. The difference between these values is a measure of the range of angles over which the fluorescent group can move relative to the macromolecule.

range of orientations, some net polarization still will be seen. Macromolecular motion will be required in order for the chromophore to experience all possible orientations. Thus, at low viscosity, the dependence of the residual polarization on $T\eta$ will reflect motion of the macromolecule as a whole. Extrapolation of this $\bar{P}$ back to $T\eta = 0$ on a plot of $\bar{P}^{-1}$ versus T/η allows a measure of the range of angles covered by fast chromophore motion.

At sufficiently high viscosities, the macromolecule is effectively stationary. The chromophore still is free to move, and its motion will be detected by an enhanced dependence of polarization on T/η at high η. The result will be a nonlinear Perrin plot, such as that shown schematically in Figure 8-25. Polarization thus can provide clear evidence of flexibility either near the binding sites of probes or of a whole macromolecular structure. This is important information that often is quite difficult to detect by translational hydrodynamic measurements such as sedimentation.

In addition to monitoring molecular motions, polarization also can be used to detect singlet–singlet energy transfer. Suppose a protein or nucleic acid contains two or more identical fluorescent chromophores. If one of these is excited, energy transfer can lead to migration of the excitation to other chromophores prior to emission. If these chromophores are not oriented parallel to the original absorber, the emitting dipole will no longer be parallel to the absorbing dipole. The polarization observed for the system will be altered as described by Equation 8-64. If the chromophores have fluorescence spectra shifted far to the red of their absorption, these effects are likely to be small because the spectral overlap will be poor, leading to small values of R_0. But many chromophores have fluorescence that substantially overlaps their absorption. In these cases, polarization measurements are an effective way to measure interchromophore distances. However, if energy-transfer effects are large, they will severely complicate efforts to measure molecular size and shape by polarization.